

Do happy catalyst supports work better? Surface coating of silica and titania supports with (poly)dopamine and their application in hydrotreating

Rajesh Munirathinam, Dorothée Laurenti, Denis Uzio, Gerhard D Pirngruber

▶ **To cite this version:**

Rajesh Munirathinam, Dorothée Laurenti, Denis Uzio, Gerhard D Pirngruber. Do happy catalyst supports work better? Surface coating of silica and titania supports with (poly)dopamine and their application in hydrotreating. Applied Catalysis A : General, 2017, 544, pp.116-125. 10.1016/j.apcata.2017.07.008 . hal-01631693

HAL Id: hal-01631693
https://ifp.hal.science/hal-01631693

Submitted on 9 Nov 2017

HAL is a multi-disciplinary open access archive for the deposit and dissemination of scientific research documents, whether they are published or not. The documents may come from teaching and research institutions in France or abroad, or from public or private research centers.

L'archive ouverte pluridisciplinaire **HAL**, est destinée au dépôt et à la diffusion de documents scientifiques de niveau recherche, publiés ou non, émanant des établissements d'enseignement et de recherche français ou étrangers, des laboratoires publics ou privés.

*Manuscript
Click here to view linked References

Do happy catalyst supports work better? Surface coating of silica and titania supports with (poly)dopamine and their application in hydrotreating

Rajesh Munirathinam, Dorothée Laurenti, Denis Uzio*, Gerhard D. Pirngruber*

IFP Energies Nouvelles (IFPEN) - Lyon, Rond-point de l'échangeur de Solaize, BP 3, 69360 Solaize, France

*Corresponding authors: Tel.: +33 437702243 (D. Uzio) / +33 437702733 (G. D. Pirngruber).

E-mail address: denis.uzio@ifpen.fr (D. Uzio) / gerhard.pirngruber@ifpen.fr (G. D. Pirngruber).

Abstract

In order to meet the demand for cleaner fuels, it is necessary to develop high performing hydrotreating catalysts. Although organic additives are often used to improve the performances of hydrotreating catalysts, bio-polymer additives have not yet been thoroughly investigated. We recently showed that dopamine, a neurotransmitter molecule, which is also frequently found in adhesive bio-polymers, efficiently coats the surface of an alumina carrier material and modifies the interaction with active components of hydrotreating catalysts, i.e. cobalt and molybdenum. The catalytic performance of the CoMoS/Al_2O_3 catalysts could, thus, be improved. In the present paper we extend the strategy to other carrier materials (silica and titania). The catalysts prepared on (poly)dopamine (Pdop) coated silica showed enhanced activity for the hydrogenation of toluene reaction and the selective HDS of FCC gasoline model feed. Pdop coating lowers the MoS_2 nanocrystallites' stacking on silica, thereby improving the accessibility of active edge sites. The origin of this increase in catalytic activity may be found in the higher capacity of Pdop's functional groups to interact with metallic precursors leading to a better dispersion of the active phase. On the contrary, when the interaction between the dopamine and the support is too strong (as observed for TiO_2), the functional groups of Pdop are not available for interaction with Co and Mo species, resulting in decreased catalytic activity.

Keywords:

Carbon coating, Hydrodesulfurization, Hydrotreating reactions, Polydopamine, Silica, Titania

Highlights:

- SiO_2 and TiO_2 surfaces were successfully coated by polydopamine (Pdop).
- CoMoS catalysts supported on Pdop/SiO_2 showed better dispersion and two-fold increase in catalytic activity than their counterparts on bare SiO_2.
- Opposite effect was observed CoMoS catalysts supported on Pdop/TiO_2.
- Nature of interaction between the support and Pdop functional groups determines the final outcome of the catalyst dispersion and their activity.

1 Introduction

Environmental regulations are continuously strengthened to limit the emission of pollutants from fossil fuels combustion [1]. In addition, natural resources supplying the metal sources for hydrotreating catalysts are limited whereas liquid fuel demand is expected to grow by 48% between 2012 and 2040 (source: International Energy Outlook 2016). These constraints drive the need to develop highly active and efficient hydrotreating catalysts. Industrial hydrotreating catalysts contain Mo (and/or W) as the active metal usually promoted by Co (and/or Ni) and supported on Al_2O_3, SiO_2 or TiO_2 [2]. In order to improve their performances, different strategies have been explored such as the use of polyoxometalates [3], or different kinds of organic additives, namely, organic chelating [4–6] or non-chelating (e.g. glycols) agents [7,8].

The support effect is an important field of investigation in hydrotreating catalysis. Indeed, metal-support interactions are known to influence various characteristics of the active phase such as its morphology, slabs orientation, or electronic properties [9–12]. Acid or basic sites on the support surface can also intervene directly in the catalytic cycle and enhance the formation of the desired products, but in many cases also promote the formation of undesired side products [13]. Silica is an interesting option when acid catalyzed reactions (olefin polymerization, coke formation, etc.) are detrimental, or when low metal support interactions are required to limit the formation of refractory phases [14,15]. However, silica-supported catalysts generally show lower activity than alumina counterparts due to the relatively inert surface making it difficult to form the highly dispersed and promoted sulfide phase, especially at high loadings. In order to circumvent such limitations, coating the surface of silica with a polymer that contains different functional groups able to interact with metallic precursors is one of the suitable option to improve surface reactivity and dispersion [16].

Titania is also a very interesting support material. Non-promoted MoS_2/TiO_2 catalysts are four to five times more active than their alumina counterparts [17]. The high activity was explained either by electronic effects, or by the epitaxial relationship between anatase and MoS_2, which leads to edge-bonded slabs that mainly expose M-edges. Yet, the promotion effect of Co on titania supported MoS_2 is weaker than the one observed on γ-Al_2O_3 for instance, because only a small fraction of Co is incorporated into the mixed CoMoS phase [9].

In a recent study from our group, we have successfully modified the surface properties of alumina carriers, by coating with the bio-molecule dopamine. Under soft conditions, a polydopamine-coated alumina was obtained [18]. The choice of dopamine monomer is (bio-)inspired from the properties of mussel adhesive proteins, on the basis of the strong interfacial binding property of embedded catechol groups [19]. Dopamine polymerizes under mild basic reactions conditions and invariably coat almost all kinds of materials such as metals, metal oxides, polymers, etc [20]. In addition, the chemical structure of polydopamine (Pdop) includes various functional groups such as catechol, quinone, amine and imine that are useful to bind many transition metal ions [21,22]. In the case of Al_2O_3, the Pdop coating of the surface prevented the direct interaction of cobalt and molybdenum species with the alumina surface (which leads to the formation of refractory species), while providing a higher number of binding sites for molybdenum precursors, leading *in fine* to an improved dispersion of the MoS_2 slabs, in particular at high surface densities of molybdenum. The combination of both effects led to an

improved activity of the CoMoS/Pdop/Al_2O_3 in the hydrogenation of toluene and also in the hydrotreating of gasoil.

In contrast to alumina, silica has a fairly weak interaction with molybdenum species. The fact that the Pdop coating provides binding sites for molybdenum is therefore a particularly interesting strategy to improve the dispersion of MoS_2 slabs on the silica surface. In the case of titania, the effect of the Pdop coating is difficult to predict, because of the very specific interaction between MoS_2 slabs and the titania surface.

In the present work, we show how SiO_2 and TiO_2 carriers can be coated by Pdop. The coated supports were characterized in detail and then used for preparation of hydrotreating catalysts, via classical incipient wetness impregnation of molybdenum and cobalt species. The performance of the sulfide catalysts in toluene hydrogenation and selective hydrodesulfurization (HDS) of 3-methylthiophene was assessed and discussed in relation with characterization results.

2 Experimental Section

2.1 Materials

All the chemicals were purchased from Sigma Aldrich and used as received unless specified. Silica and titania (anatase) supports were provided by Saint-Gobain and Huntsman, respectively. The shaping of the titania supports was done in-house.

2.2 Support modification

SiO_2 support (1.6 mm diameter cylindrical extrudates, V_p = 1.10 cm^3g^{-1}, S_{BET} = 233 m^2g^{-1}, d_p = 12.9 nm) was coated with Pdop by incipient wetness impregnation. The desired amount of dopamine-hydrochloride was dissolved in water and impregnated onto SiO_2. Impregnation was followed by a maturation step in a water saturated atmosphere, for overnight at room temperature. Then, a drying step was performed for 20 h at 90°C which yielded Pdop coated silica (Pdop/SiO_2). The drying step helps in polymerizing dopamine [23] partially, as observed by the change in color of the support from white to brown. A similar approach was used to coat titania (1.6 mm diameter trilobe extrudates, V_p = 0.63 cm^3g^{-1}, S_{BET} = 173 m^2g^{-1}, d_p = 17.2 nm) with Pdop to obtain Pdop/TiO_2. Pdop coated TiO_2 is an orange solid. Pdop/SiO_2 and Pdop/TiO_2 supports used for the catalyst preparation contain Pdop loading of 13.8 wt% on SiO_2 and 6.4 wt% on TiO_2.

2.3 Catalyst preparation

Series of CoMo/Pdop/SiO_2 and CoMo/SiO_2 catalysts with 10 or 20 wt% loading of MoO_3 (with respect to the oxide form of the catalysts) and Co/(Co+Mo) molar ratio of 0.3 were prepared by incipient wetness impregnation method and labelled as 10(20)%CoMo/Pdop/SiO_2 and 10(20)%CoMo/SiO_2. Phosphomolybdic acid ($H_3PMo_{12}O_{40}.30H_2O$) and $Co(NO_3)_2.6H_2O$ were used as precursors dissolved in ethanol. The solution containing the metal precursors was impregnated and left for maturation in an ethanol saturated atmosphere, at room temperature

overnight. Then, the catalysts were dried in a rotary evaporator under reduced pressure (~50 mbar) for 2 h at 40°C which yielded CoMo/Pdop/SiO_2 or CoMo/SiO_2. 10%CoMo/Pdop/TiO_2 and 10%CoMo/TiO_2 catalysts were also prepared using the same method described above. The catalysts were sulfided in gas-phase at atmospheric pressure before characterization. For sulfidation, catalysts were introduced in a glass reactor and heated from room temperature to 350°C with a ramp of 5°C min^{-1} with a plateau of 2 h, under a 15:85 v/v H_2S/H_2 flow of 1.8 L $g^{-1}_{catalyst}$ h^{-1}. At the end of the plateau, the reactor was cooled down to 50°C and the H_2S/H_2 mixture was replaced by argon and the reactor was flushed for 15 min. Finally, the reactor was evacuated (~1 mbar) and the cell was sealed. The sulfided catalysts are henceforth denoted as CoMoS/Pdop/(TiO_2)SiO_2 and CoMoS/(TiO_2)SiO_2.

2.4 Catalysts characterization

Fourier transform infrared spectroscopy (FTIR), thermogravimetric analysis (TGA), textural, elemental (XRF and CHNS), *in-situ* XRD, electron probe microprobe analysis (EPMA), transmission electron microscopy (TEM), and X-ray photoelectron spectroscopy (XPS) analysis were performed as described before [18]. The results of elementary analysis are presented in Table 1. Targeted MoO_3 loadings were based on the oxide form of the bare support.

Table 1
%wt of (i) Mo and Co in the catalyst before sulfidation from XRF analysis, and (ii) C and S in the sulfide catalysts from CHNS analysis.

Catalysts	Targeted MoO_3 wt%	Mo wt%	Actual MoO_3 wt%[a]	Co wt%	S wt%	C wt%
10%CoMo/SiO_2	10	5.7	8.5	1.5	5.9	n.d.
10%CoMo/Pdop/SiO_2	10	6.0*	9.0*	1.6*	5.5	5.3
20%CoMo/SiO_2	20	10.6	15.8	2.8	11.0	n.d.
20%CoMo/Pdop/SiO_2	20	11.9*	17.8*	3.1*	10.4	2.4
10%CoMo/TiO_2	10	5.4	8.1	1.8	7.2	n.d.
10%CoMo/Pdop/TiO_2	10	4.8	7.1	1.5	6.4	0.9

* MoO_3 and CoO contents of these catalysts are from the sulfided catalysts. n.d. not detected. [a]MoO_3 wt% was calculated from the measured Mo wt% from XRF.

2.4.1 Solid state UV analysis

A double-beam Lambda 35 UV-Vis spectrophotometer from Perkin-Elmer equipped with an integrating Lab sphere RSA-PE-20 recording the spectra over 200-1000 nm range was used with a data interval of 2 nm. The spectra were recorded in reflectance mode. The parameters used were 4 nm s^{-1} as scan speed and 2 nm as slit width. Spectralon was used as a reference. Samples were prepared by mixing 10 mg of pure sample with 190 mg of $BaSO_4$.

2.5 Catalytic tests

2.5.1 Hydrogenation of Toluene

The sulfided catalysts were evaluated in toluene hydrogenation (HYD) reaction in a fixed bed unit reactor *Flowrence* (*Avantium*), containing 16 parallel reactors, filled with 450 µL µL of the catalyst, as described before [18]. Briefly, the feed was composed of dimethyldisulfide (DMDS, 5.8 wt%) and toluene (20 wt%) in cyclohexane (74.2 wt%). The hydrogen to feed ratio (H_2/HC) was 450 NL/L during the test and the *in-situ* presulfidation step, which was performed at 350°C with a liquid hourly space velocity (LHSV) of 4 h^{-1} and a total pressure of 60 bar for 2 h. After this presulfidation step, LHSV was reduced to 2 h^{-1}. The first order rate constant (*k,* h^{-1}) was calculated by the following expression (1):

$$k = LHSV * \ln\left(\frac{1}{1-x}\right), LHSV = \frac{flow\ rate\ of\ the\ feed}{volume\ of\ the\ catalytic\ bed}, k' = \frac{k}{mol(Mo)} \quad (1)$$

x is the percentage conversion of toluene (HYD) in the feed. LHSV is the liquid hourly space velocity (h^{-1}). *k′* ($cm^3\ mol_{Mo}^{-1}\ h^{-1}$) is obtained by normalizing *k* with the number of moles of Mo present in the catalyst loaded in the test.

2.5.2 HDS of 3-methylthiophene (3-MT) and hydrogenation (HYD) of 2,3-dimethyl-2-butene (2,3-DM2B): Model FCC gasoline feed test

The catalysts were also evaluated in selective HDS of model FCC gasoline test in the *Flowrence* unit from *Avantium,* using circa 300 µL of catalyst in each fixed bed reactor. The presulfidation of the catalysts was performed using a feed composed of DMDS (4 wt%) in n-heptane (96 wt%), at a LHSV of 3 h^{-1}, at a total pressure of 15 bar, for 2 h, and with a hydrogen to feed ratio (H_2/HC) of 300 NL/L. The temperature was increased from room temperature to 350°C with a ramp of 2°C min^{-1}. After the sulfidation step, the temperature was decreased to 190°C. The catalytic test was carried out with a feed composed of 2,3-DM2B (10 wt%), and 3-MT (0.3 wt%) dissolved in n-heptane (89.7 wt%), at a LHSV of 6 h^{-1}, with total pressure of 15 bar, and the hydrogen to feed ratio (H_2/HC) of 300 NL/L. Later, the temperature was increased from 190 to 220°C with an increment of 10°C. The liquid products of the reaction were analyzed by gas chromatography using a DB1 column. The first order rate constant (*k,* h^{-1}) was calculated by the following expression (2):

$$k(HDS\ or\ HYD) = LHSV * \ln\left(\frac{1}{1-X_{HDS\,(HYD))}}\right) \quad (2)$$

x is the conversion of 3-MT (HDS) or the hydrogenation of 2,3-DM2B (HYD). As previously described, *k′* ($cm^3\ mol_{Mo}^{-1}\ h^{-1}$) is obtained by normalizing *k* with the number of moles of loaded Mo.

3 Results and Discussion

3.1 Coating of silica support with Pdop

3.1.1 Fourier Transform Infrared Spectroscopy (FTIR)

FTIR spectra of the SiO_2 and Pdop/SiO_2 supports prepared by impregnating the carrier with 6.4 or 13.8 wt% of dopamine-hydrochloride are shown in Fig. 1. The sharp peak at 3747 cm^{-1} corresponds to stretching vibrations of the isolated surface silanol (SiOH) groups on silica support [24]. This signal drops when Pdop loading increases, and at 13.8 wt% of Pdop, the majority of the free OH groups on SiO_2 has disappeared (Fig. 1c). Infrared bands between 1650 and 1400 cm^{-1} represent the vibration modes of aromatic rings indicative of the presence of single or condensed aromatic rings [25]. The band corresponding to ammonium ion (~1612 cm^{-1}) stretching from dopamine-hydrochloride salt (Fig. 1d) has almost disappeared on Pdop/SiO_2 (Fig. 1b and 1c), indicating the transformation of the salt form of dopamine. Further, drying conditions (90°C for 20 h) helped to polymerize dopamine at least partially [23], as witnessed from the transformation of color from white to brown.

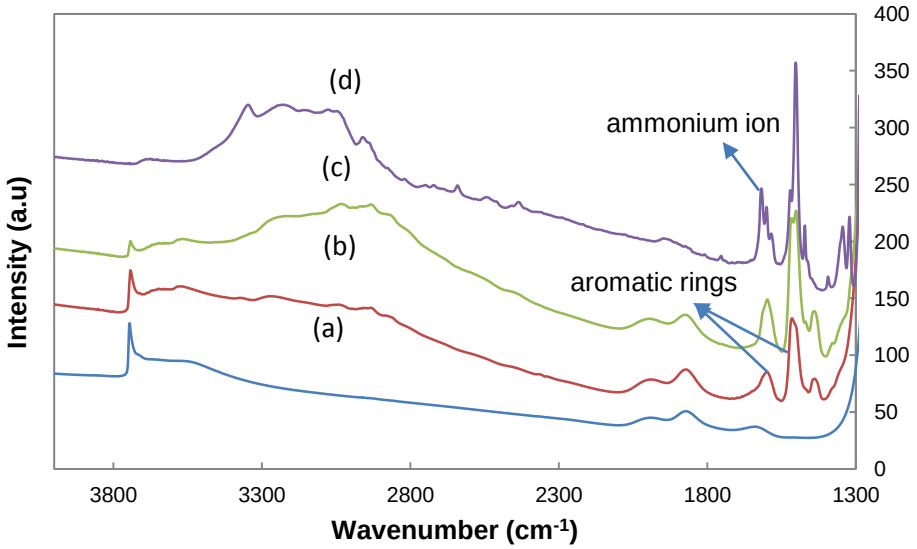


Fig. 1. FTIR spectra of (a) SiO_2, (b) 6.4 wt%Pdop/SiO_2, (c) 13.8 wt%Pdop/SiO_2, and (d) dopamine-hydrochloride after activating the samples at 90°C for 2 h.

3.1.2 Thermogravimetric and Solid-state UV analysis

The thermal degradation profiles of 6.4 wt%Pdop/SiO_2 and 13.8 wt%Pdop/SiO_2 are depicted in Fig. 2. The free dopamine-hydrochloride decomposes at about 330°C (Fig. S1), whereas 6.4 wt%Pdop/SiO_2 and 13.8 wt%Pdop/SiO_2 decomposes only partially at 330°C. The partial decomposition at 330°C reveals the presence of free or unpolymerized dopamine. However, the decomposition behavior continues up to 700°C. This is a clear indication of the presence of polymerized/oligomerized dopamine, which undergoes thermal degradation at temperatures higher than 330°C. Further, solid-state UV analysis of the Pdop/SiO_2 support (Fig. S2) showed

an absorbance band at about 280 nm corresponding to catechol groups of dopamine [19]. In addition, an increase in absorbance in the region of 400-800 nm which is characteristic for the polymerization of dopamine, arising from different functional groups in Pdop was also observed [26].

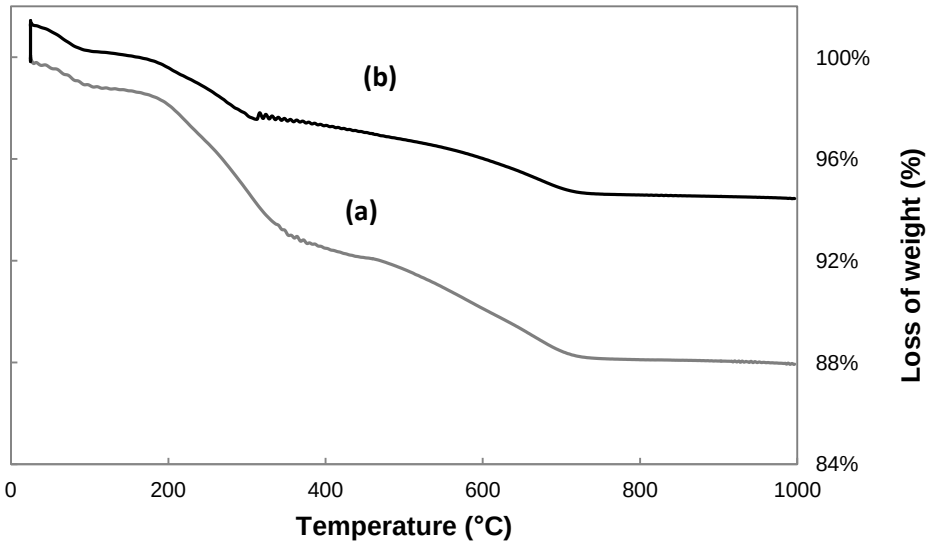


Fig. 2. Thermogravimetric analysis of (a) 6.4 wt%Pdop/SiO_2, and (b) 13.8 wt%Pdop/SiO_2 supports under H_2 gas.

3.1.3 Textural Analysis

Nitrogen physisorption isotherms of SiO_2 and 13.8 wt%Pdop/SiO_2 supports are displayed in Fig. 3 (while usual BET surface area, pore volume and pore diameter are presented in Table S1). The amount of adsorbed N_2, normalized by the volume of the support [27] (obtained by multiplying the grain density with the weight of the carrier), does not change much when SiO_2 is coated with 13.8 wt%Pdop. This indicates that the dopamine coating does not reduce the pore volume. The shape of the isotherm is preserved, corresponding to type IV with H1 hysteresis before and after Pdop coating. The N_2 isotherms suggests that we obtain a homogeneous coating of the surface, with no pore blocking effect.

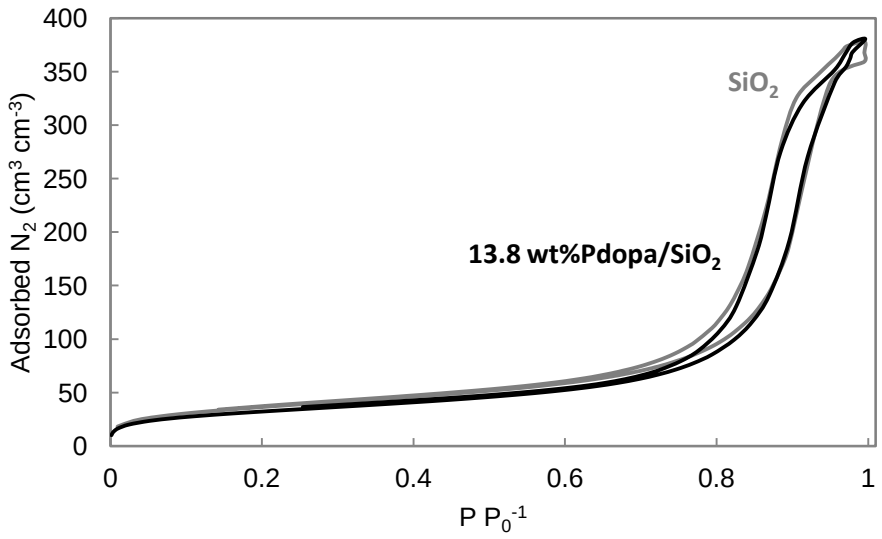


Fig. 3. N_2 physisorption isotherms of SiO_2 and 13.8 wt%Pdop/SiO_2.

3.2 CoMo supported on Pdop coated SiO_2

Both the pure and Pdop modified silica supports were impregnated with Mo and Co precursors using ethanol as the solvent as described in the experimental section. These catalysts were characterized by electron probe microanalysis to analyze the distribution of metal precursors within the extrudates. Distribution profiles of Mo, Co, and P in the cross section of 20%CoMo/Pdop/SiO_2 and 20%CoMo/SiO_2 extrudates (Figs. S3-S4) in the oxide form of the catalysts showed that all the elements were homogeneously distributed. CHNS analysis results (Table 1) obtained on the CoMoS/13.8 wt%Pdop/SiO_2 catalysts showed that part of the carbon from Pdop (2.4 to 5.3 wt%) is still present after sulfidation. N_2 physisorption measurements on 20%CoMoS/SiO_2 and 20%CoMoS/Pdop/SiO_2 sulfided catalysts displayed no significant difference for the adsorbed N_2 volume (Figs. S5-6, See Table S1 for usual BET surface area, pore volume and pore diameter). It is important to note that despite of the presence of carbonaceous deposit after sulfidation, no pore blocking effect is detected in this study, in contrast to other studies on carbon coated supports reported in literature [28,29].

3.2.1 XRD analysis: In-situ sulfidation of CoMo catalysts supported on SiO_2 and Pdop/SiO_2

The sulfidation of Mo and Co supported on SiO_2 and Pdop/SiO_2 (20 wt% of targeted MoO_3 loading) was analyzed *in-situ* by XRD, to follow the formation of MoS_2 and Co_9S_8 crystalline phases with the increase in temperature (Fig. 4). The formation of a crystalline MoS_2 phase begins gradually on both supports above 200°C. The increase in the intensity of the XRD reflections with temperature follows a similar trend for both supports, showing that the Pdop coating does not modify significantly the formation and growth of sulfide crystals, despite the complexation of Mo ions with catechol groups in Pdop (Figs. 4a and 4b) [30]. The height of the (002) peak calculated from Debye-Scherrer equation for crystalline MoS_2 was used to get information about the stacking of MoS_2 slabs on both supports [31]. The (002) peak of MoS_2 is

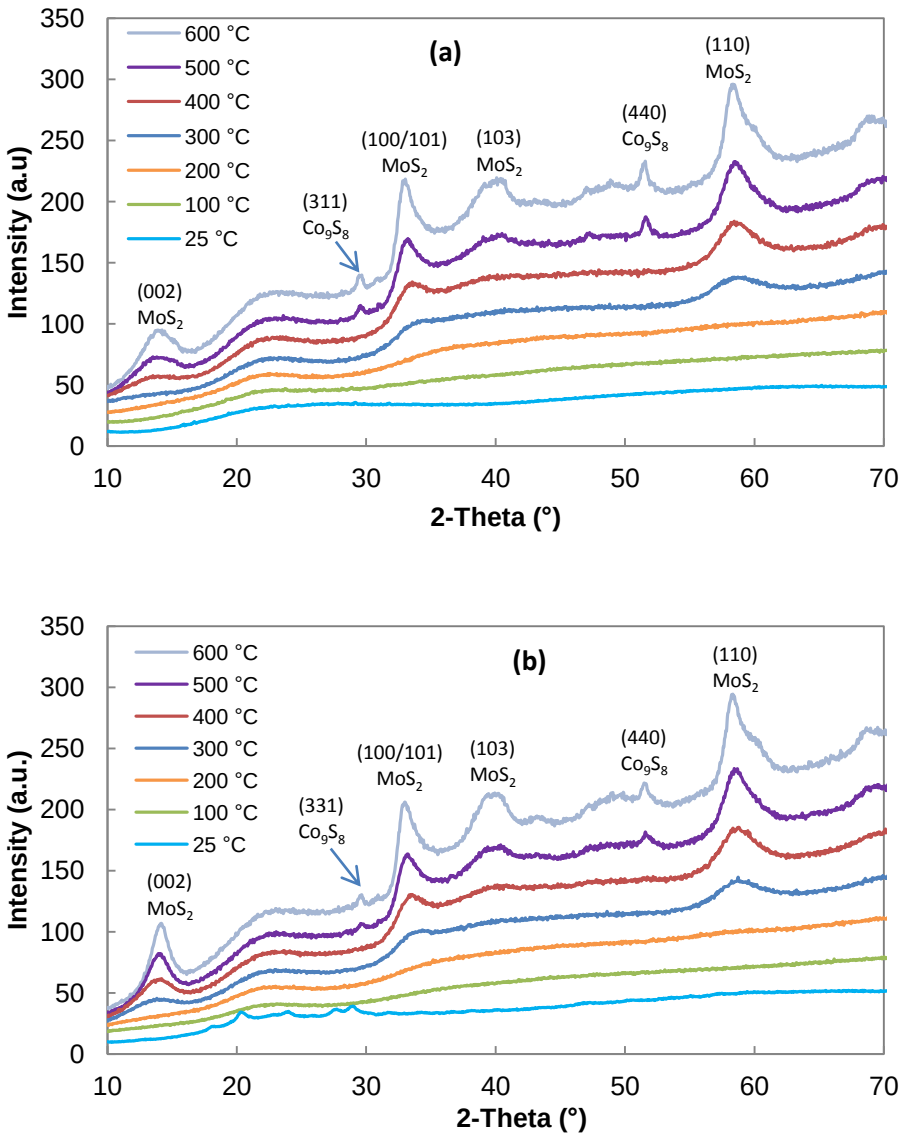


Fig. 4. XRD diffraction patterns of MoS_2 and Co_9S_8 phases on (a) Pdop/SiO_2 and (b) pure SiO_2 obtained during *in-situ* sulfidation of the oxide catalysts.

broader and has a lower intensity on Pdop/SiO_2 (Fig. 4a) than on pure SiO_2 (Fig. 4b), i.e. the MoS_2 stacking on the Pdop/SiO_2 support is lower (Fig. S7, considering the Mo-Mo d-spacing of (002) crystal plane as 6.5 Å for a single MoS_2 layer [32]). Since stacking and dispersion are generally anti-correlated, MoS_2 slabs are expected to be more dispersed on Pdop/SiO_2 than on pure SiO_2. The formation of a crystalline Co_9S_8 phase starts above 400°C, and follows a similar trend for both pure SiO_2 and Pdop/SiO_2. Above 400°C, it is most likely that the Co ions present in the CoMoS starts to segregate from the sintering MoS_2 slabs (which reduces the amount of Co that can decorate the edges of the slabs) and form the thermodynamically stable Co_8S_9 phase.

3.2.2 TEM results

The mean slab length and stacking of MoS_2 nanocrystallites were determined from a statistical treatment of the TEM images. At both low and high Mo loadings, the stacking of the MoS_2 slabs on Pdop/SiO_2 is significantly lower than on the corresponding bare SiO_2 supports (See Figs. 5 and 6, and Table 2) in agreement with previous XRD results. The representative TEM micrographs reveal that, on pure SiO_2, more aggregation/clusters of MoS_2 slabs are observed (dark zones on representative images at low and high magnifications, Figs. 5a-b), compared to the Pdop-coated support (representative images, Figs. 5c-d). The impact of dopamine on the average slab length is less obvious since it slightly decreases at low Mo loading, but marginally increases at high Mo loading (Table 2).

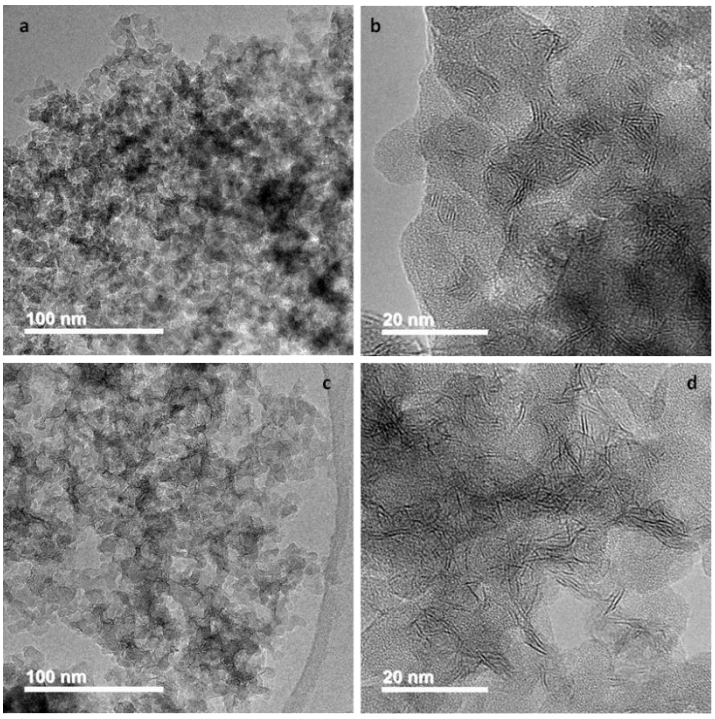


Fig. 5. TEM images of sulfided catalysts: a-b) 20%CoMoS/SiO_2 and c-d) 20%CoMoS/Pdop/SiO_2.

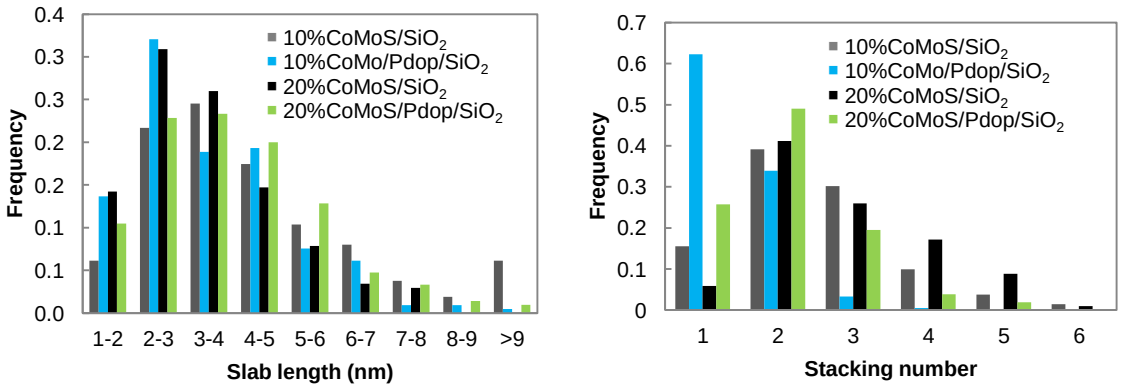


Fig. 6. Distributions of (a) slab length and (b) average stacking of the MoS_2 particles in the CoMoS catalysts supported on SiO_2 and Pdop/SiO_2 determined by TEM.

Table 2
Average slab length and stacking CoMoS catalysts supported on SiO_2 and Pdop/SiO_2 determined by TEM. The ± interval indicates the width of the distribution and not the uncertainty of the average slab length and stacking.

Catalysts	Slab length (nm)	Average Stacking
10%CoMoS/SiO_2	4.7 ± 2.2	2.5 ± 1.1
10%CoMoS/Pdop/SiO_2	3.8 ± 1.5	1.4 ± 0.6
20%CoMoS/SiO_2	3.7 ± 1.5	2.9 ± 1.1
20%CoMoS/Pdop/SiO_2	4.2 ± 1.7	2.1 ± 0.9

3.2.3 XPS results on CoMoS catalysts supported on SiO_2 and Pdop/SiO_2

The binding energies of Mo and Co ions in the sulfided (CoMoS) catalysts with/without Pdop were evaluated by XPS. In the case of Mo, the XPS spectra allow distinguishing MoS_2, MoO_3 and a species with an intermediate binding energy, a Mo-oxysulfide. Results from XPS (Table 3) do not show any observable difference in the degree of sulfidation of Mo ions for all the catalysts (both at low and high Mo loadings). However, at 10% MoO_3 loading, the amount of Co_9S_8 phase is much lower on Pdop/SiO_2 when compared to that on pure SiO_2, consequently, increasing the decoration ratio of MoS_2 slabs by Co, i.e. the CoMoS phase (+ 57%). On the contrary, at high Mo loading, there is no significant difference in the distribution of Co ions present on pure SiO_2 and Pdop/SiO_2.

Table 3
Metal distribution for cobalt and molybdenum species present at the surface of sulfided CoMoS supported on SiO_2 and 6.4 wt%Pdop/SiO_2 obtained from XPS analysis.

	Atomic Ratio	Mo species (% relative)			Co species (% relative)			S species (% relative)		Atomic ratio
Catalyst	Co:Mo Slabs	MoS_2	MoO_xS_y	Mo^{+VI}	Co_9S_8	CoO	CoMoS	S_{Sulf}	S_{Ox}	Co:Mo total
10%CoMoS/SiO_2	0.17	77	13	10	52	25	23	84	16	0.58
10%CoMoS/Pdop/SiO_2	0.28	78	13	9	38	26	36	86	14	0.61
20%CoMoS/SiO_2	0.34	78	13	9	24	31	45	88	12	0.59
20%CoMoS/Pdop/SiO_2	0.29	78	13	9	25	29	46	87	13	0.49

3.3 Catalytic tests on SiO_2- and Pdop/SiO_2-supported catalysts.

3.3.1 Hydrogenation of toluene

At both low and high Mo loadings, the conversion of toluene using the Pdop/SiO_2 support increases by 30-40% when compared with the catalysts supported on pure SiO_2 (Fig. 9). Consequently, the corresponding first order rate constants normalized per mole of Mo loaded in

the reactor (*k'*) increased by a factor of about 1.5 to nearly 2 showing a large increase of the intrinsic activity. At high Mo loading, *k'* decreases on both Pdop/SiO_2 and pure SiO_2, indicating that the active catalytic sites does not increase proportionally with the Mo content.

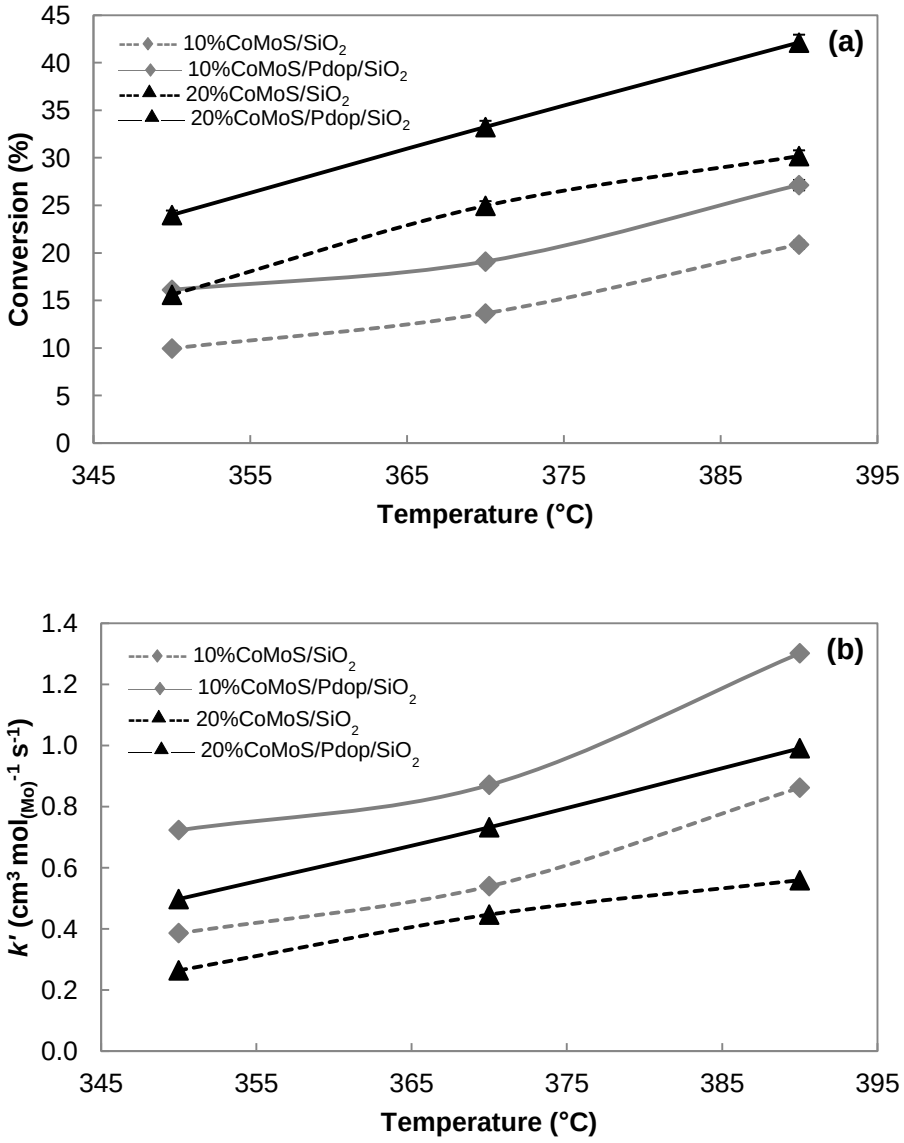


Fig. 9. (a) Conversion and (b) first-order rate constants (*k'*) normalized by the moles of Mo in the catalysts for toluene hydrogenation at 350, 370 and 390°C using 10 and 20 wt% of targeted MoO_3 loading on Pdop/SiO_2 and SiO_2.

3.3.2 HDS of 3-methylthiophene (3-MT) versus HYD of 2,3-dimethyl-2-butene (2,3-DM2B)

Selective removal of sulfur from (benzo)thiophene derivatives while avoiding the hydrogenation of olefins (HYD), is a key requirement in the selective FCC gasoline hydrotreating. The competitive conversion of 3-MT (HDS) versus HYD of 2,3-DM2B is used as a test reaction to evaluate the different CoMoS catalysts. At both low and high Mo loading, CoMoS

catalysts supported on 13.8 wt%Pdop/SiO_2 showed an increase in the conversion by a factor of about two for both HDS and HYD reactions compared to their counterparts supported on pure SiO_2. For both low and high Mo loadings, the first order rate constants (*k'*, Table 4) for 3-MT conversion using CoMoS supported on Pdop/SiO_2 increased by a factor of about 2 when compared to that of CoMoS on pure SiO_2. The *k'* for HYD of 2,3-DM2B increased by a factor of about 2.5 to 3 (Table 4). Selectivity graph for the conversions of 3-MT and HYD of 2,3-DM2B is presented in Fig. 10. The selectivity for 3-MT conversion is slightly decreased at low Mo loading, whereas, at high Mo loading the selectivity is intact. That means Pdop allows to increase the activity without any significant loss of selectivity which is quite unusual.

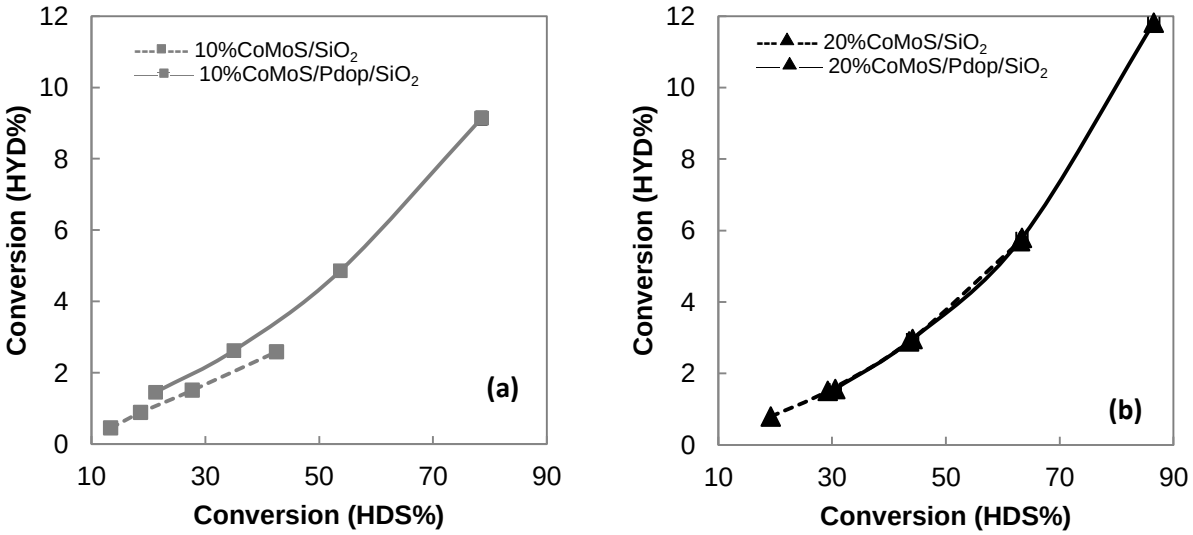


Fig. 10. Conversion in HYD of 2,3-dimethyl-2-butene versus conversion of 3-methylthiophene at 190, 200, 210 and 220°C using a) 10 wt% and b) 20 wt% of targeted loading on Pdop/SiO_2 and SiO_2.

Table 4
First order rate constants normalized by moles of Mo in the catalyst (*k'*) for HDS of 3-MT and 2,3-DM2B for the CoMoS catalysts supported on SiO_2 and Pdop/SiO_2.

Catalysts	*k*' (HDS) ($cm^3\ mol_{(Mo)}^{-1}\ h^{-1}$)				*k*' (HYD) ($cm^3\ mol_{(Mo)}^{-1}\ h^{-1}$)			
	190 °C	200 °C	210 °C	220 °C	190 °C	200 °C	210 °C	220 °C
10%CoMoS/SiO_2	2.91	4.18	6.59	11.24	0.09	0.18	0.31	0.53
10%CoMoS/Pdop/SiO_2	4.31	7.79	13.92	27.80	0.26	0.48	0.90	1.73
20%CoMoS/SiO_2	1.49	2.42	4.00	6.96	0.06	0.11	0.21	0.41
20%CoMoS/Pdop/SiO_2	2.90	4.64	7.99	15.95	0.13	0.24	0.47	1.00

3.4 CoMo supported on Pdop coated titania and its catalytic activity

Pdop/TiO_2 was prepared by impregnating the carrier with 6.4 wt% of dopamine-hydrochloride. The FTIR spectrum showed that the peak around 3600 cm^{-1} corresponding to stretching vibrations of the hydroxyl groups on TiO_2 support [33] considerably decreased upon Pdop coating (Fig. S8), evidencing the modification of titania surface by Pdop. The results from thermogravimetric analysis showed partial polymerization of dopamine (Fig. S9), similar to that on Pdop/SiO_2 (Fig. S1). In addition, Pdop/TiO_2 appeared in orange color, in contrast to the black or dark brown color (typical color for Pdop) for Pdop/Al_2O_3 and Pdop/SiO_2. It is well documented in literature that titania binds strongly with the catechol groups of dopamine in a bidentate geometry [34]. The solid-state UV analysis of the Pdop/TiO_2 support showed the ligand-to-metal charge transfer complex formation between TiO_2 and catechol groups [35] extended the absorption into the visible light region as apparently indicated by the color change (Fig. S10).

As previously described, the Pdop/TiO_2 and bare TiO_2 supports were impregnated with Mo and Co precursors (10 wt% of targeted MoO_3 loading) using ethanol as the solvent. TEM analysis (Figs. S11-12 and Table S2) revealed that the dopamine-coating increases the mean slab length of MoS_2 nanocrystallites (from 3.1 nm on bare TiO_2 to 3.7 nm on Pdop/TiO_2). The stacking of MoS_2 slabs (~1.6) was similar on both supports. It can be concluded from TEM results that the number of exposed edge atoms of MoS_2 decreases with the addition of Pdop. XPS study (Table S3) showed that the degree of sulfidation of Mo ions on Pdop/TiO_2 (77 %) is slightly better when compared that on bare TiO_2 (68 %). However, the percentage of catalytically inactive Co_9S_8 phase is somewhat higher on Pdop/TiO_2 (11%) when compared to pure TiO_2 (4%).

The conversion of toluene using CoMoS catalysts with Pdop was lower than the catalysts on pure TiO_2 and, the corresponding first order rate constants normalized per mole of Mo loaded in the reactor (*k'*) were reduced by 20-30% (Fig. 11).

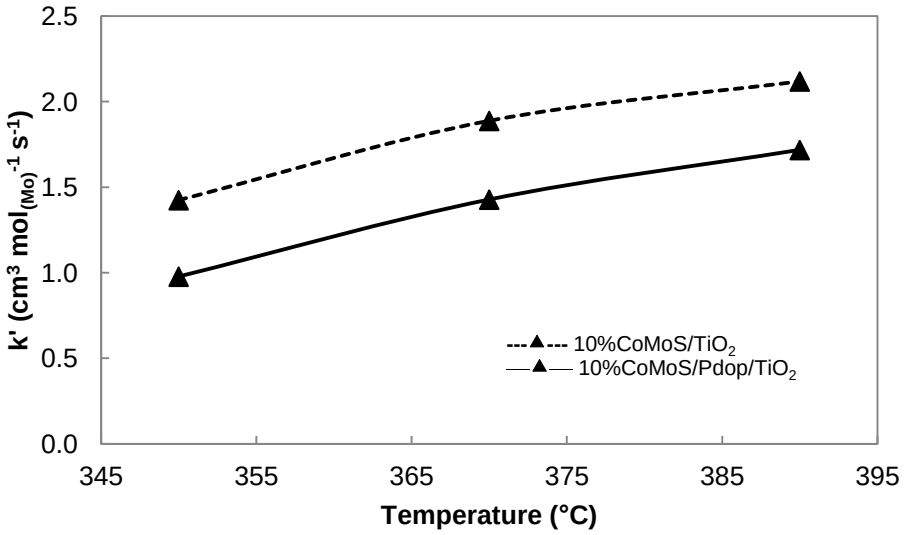


Fig. 11. First-order rate constants (*k'*) normalized by the moles of Mo in the catalysts for toluene hydrogenation at 350, 370 and 390°C using 10 wt% of targeted loading of MoO_3.

3.5 Discussion

3.5.1 Coating of oxide carriers by dopamine: Al_2O_3 vs. SiO_2 vs. TiO_2

Dopamine polymerizes easily on Al_2O_3, since the point of zero charge (PZC) of this amphoteric support is about pH 9. Al_2O_3 surface hydroxyls act as basic groups when contacting with the slightly acidic dopamine solution, raising the pH to mild basic conditions required for dopamine polymerization. As a result, Pdop covers the surface of Al_2O_3, further preventing the interaction of metallic precursors with surface OH groups [18]. In the case of SiO_2, dopamine is not expected to polymerize as it was observed in the case of Al_2O_3, because the PZC of SiO_2 is about pH 3 far from the basic conditions required for total polymerization. Nevertheless, it has been shown by FTIR that dopamine moieties cover the surface silanol groups. Further, TGA and UV-Vis measurements showed a partial polymerization, likely to occur during drying step in the presence of oxygen from air [23]. The degree of polymerization of dopamine is lower on silica than on alumina as evidenced from TGA and UV-Vis analysis (Fig. S2). A similar behavior is observed for TiO_2, even though its PZC is in the range of pH 5-6.

When Mo precursors are added to Pdop coated Al_2O_3 or SiO_2, the catechol groups present in Pdop form a complex with the Mo ions [30]. Consequently, Mo is distributed evenly on the Pdop coated surface of the support. However, in the case of TiO_2, there is a strong bidentate complex formation between the catechol groups of dopamine and Ti^{+IV} [34]. This strong complexation is much less pronounced for Al_2O_3 and SiO_2 supports. Hence, Pdop functional groups are available to interact with metallic precursor helping the dispersion. On the other hand, on TiO_2 due to strong complexation with Ti^{+IV}, these groups are no longer able to stabilize Mo precursors leading to sintering of MoS_2 crystallites. Further, from FTIR spectra of Al_2O_3, SiO_2, and TiO_2 at similar Pdop loading (6.4 wt%), it was observed that the contribution from catechol (OH) groups above 3300 cm^{-1} is considerably lower on TiO_2 when compared than on Al_2O_3 and SiO_2 (Fig. S13), in agreement with the above hypothesis. Convincingly, the nature of the interaction between the support and the Pdop functional groups plays a decisive in improving the dispersion of the MoS_2 crystallites.

3.5.2 Effect of Pdop coating on catalytic activity

CoMoS catalysts supported on Pdop/SiO_2 were systematically more active in the hydrogenation of toluene and FCC gasoline model molecules than the catalysts supported on bare SiO_2. The higher activities of the catalysts supported on Pdop/SiO_2 could arise from different factors, which are discussed in the following.

In our previous study, CoMoS supported on Pdop/Al_2O_3 also showed enhancement in catalytic activity mainly due to the better dispersion of MoS_2 slabs and the prevention of direct detrimental metal support interaction, owing to the presence of carbon adlayer between the support and metal [18]. Comprehensively, a similar explanation holds true in the case of CoMoS/Pdop/SiO_2. The low metal-support interactions of SiO_2 favor the stacking of MoS_2 sheets [36]. The Pdop coating significantly reduced the stacking (revealed by *in-situ* XRD and TEM measurements), at both low and high Mo loadings (Table 2). This behavior is quite unusual. Carbon-coated supports generally show higher stacking number when compared to the bare support due to the poor interaction of the carbon interface and the metal precursors [37]. With a

Pdop coating, the stacking effect has been circumvented: thanks to the presence of Pdop functional groups, MoS_2 slabs are more regularly distributed on the surface of silica support converting a poor dispersing oxide surface into a highly dispersing carbonaceous deposit. Though the degree of polymerization is lower on silica than on alumina, the catalytic activity is consistently higher on both silica and alumina, indicating polymerization is not a critical factor in improving the catalytic efficiency. We presume that the better dispersion on the support surface is the main reason for the observed increase in catalytic activity.

The presence of carbon in the sulfided CoMo on Pdop/SiO_2 could also lead to enhancement in catalytic activity. On Pdop coated SiO_2, Mo ions complexes with catechol groups present in Pdop [30]. Upon sulfidation though the complex decomposes, but still leaves carbonaceous deposit in the catalyst (at least 40% of carbon from the initial carbon content in Pdop) even after sulfidation step, with no pore blocking effect and keeping textural properties intact. This carbon is most probably present as an adlayer on SiO_2, thereby avoiding direct contact of MoS_2 nanocrystallites with SiO_2. Consequently, now MoS_2 is most possibly present on carbon like support. CoMoS phase on carbon supports generally belongs to type-II [16,38], which is characterized by weak van der Waals' interactions between the active sulfide and the support and a high intrinsic activity.

There was no direct evidence observed for an increase of Co-promoted edge sites [39] (CoMoS from XPS) on Pdop/Al_2O_3, which would contribute to the increase in catalytic inactivity. At low Mo loading, the MoS_2 slab length was reduced (TEM results, Table 2) and the degree of promotion was enhanced on Pdop/SiO_2 leading to an increase in CoMoS (+ 57%) sites (XPS results, Table 3) compared to pure SiO_2. However, these features were not observed on Pdop/SiO_2 with high Mo loading. Therefore, it is not expected to be the primary reason for the increase in catalytic activity.

The poor performance of catalysts supported on Pdop/TiO_2 could be attributed to the following factors: (i) catechol groups on dopamine form strong bonds with Ti and that causes change in the electronic properties of TiO_2, owing to the direct catechol-to-TiO_2 charge transfer [40], (ii) as catechol groups binds to titania, the number of binding sites for Mo decreases that led to the sintering of MoS_2 nanocrystallites, (iii) results from TEM showed that the MoS_2 slab length strongly increases on Pdop/TiO_2, which eventually decreases the active phase on the edge sites of MoS_2 slabs, and (iv) XPS results showed that percentage of Co_9S_8 phase on Pdop/TiO_2 is higher, as a result, the number of Co ions decorating the edge sites of MoS_2 slabs is smaller.

4 Conclusion

In conclusion, we have demonstrated a bio-inspired, facile method to coat SiO_2 and TiO_2 with Pdop. The nature of the interaction between the support and the Pdop functional groups plays a key role in the dispersion of the MoS_2 crystallites. On Pdop/SiO_2, as there is no strong interaction between the support and Pdop, functional groups on Pdop helps in dispersing metal precursors. *In-situ* XRD measurements and TEM analysis confirmed that majority of MoS_2 slabs are present in the catalysts as single or double slabs resulting in better repartition on Pdop/SiO_2

than on pure SiO_2. Despite of the presence of carbon residues in the sulfided catalysts, textural properties were intact, indicating the homogeneous deposition on the surface of the support. The CoMoS catalyst on Pdop coating increases the first order rate constants (*k'*) for toluene hydrogenation, conversions of 3-MT, and HYD of 2,3-DM2B by a factor of about 2 than its counterpart on pure SiO_2. The improved activity is attributed to the decreased aggregation of MoS_2 nanocrystallites leading to increase in edge site accessibility, and to the presence of carbonaceous adlayer between the active phase and the support limiting the direct interaction of metal precursors with the support. This coating strategy was less successful on TiO_2 owing to the stronger interaction of Pdop with titania decreasing its ability to disperse Mo active phase, consequently, decrease in catalytic activity. This point highlights the need for the appropriate interactions of the (oxidic carrier/Pdop/metallic precursors) system which have to be tuned in order to improve the final catalytic performances.

5 Acknowledgements

Anne Boffo is thanked for the technical help in the laboratory. Sylvain Carbonneaux, Mickaël Rivallan, Anne-Sophie Gay, Christèle Legens and their technical teams are acknowledged for XRF, FTIR, XRD, TEM, and XPS measurements. We are grateful for Mathieu Vidalie for his support in performing catalytic tests. We express our gratitude to Eric Puzenat for his assistance with solid state UV-VIS analysis.

6 References

[1] A. Stanislaus, A. Marafi, M.S. Rana, Catal. Today 153 (2010) 1-68.
[2] H. Toulhoat, P. Raybaud, Catalysis by transition metal sulphides: From molecular theory to industrial application, Editions Technip, Paris, 2013.
[3] R. Wang, G. Zhang, H. Zhao, catal. Today 149 (2010) 117-121.
[4] K. Hiroshima, T. Mochizuki, T. Honma, T. Shimizu, M. Yamada, Appl. Surf. Sci. 121-122 (1997) 433-436.
[5] L. Coulier, V. de Beer, J. van Veen, J.W. Niemantsverdriet, Top. Catal. 13 (2000) 99-108.
[6] Y. Ohta, T. Shimizu, T. Honma, M. Yamada, Stud. Surf. Sci. Catal. 127 (1999) 161-168.
[7] T.S. Nguyen, S. Loridant, L. Chantal, T. Cholley, C. Geantet, Appl. Catal. B: Environ. 107 (2011) 59-67.
[8] D. Nicosia, R. Prins, J. Catal. 229 (2005) 424-438.
[9] M. Breysse, P. Afanasiev, C. Geantet, M. Vrinat, Catal. Today 86 (2003) 5-16.
[10] C. Roukoss, D. Laurenti, E. Devers, K. Marchand, L. Massin, M. Vrinat, Comptes Rendus Chimie 12 (2009) 683-691.
[11] Y. Sakashita, Surf. Sci. 489 (2001) 45-58.
[12] A. Nogueira, R. Znaiguia, D. Uzio, P. Afanasiev, G. Berhault, Appl. Catal. A: Gen. 429-430 (2012) 92-105.
[13] G. Pérot, Catal. Today 86 (2003) 111-128.
[14] V. La Parola, G. Deganello, C. Tewell, A. Venezia, Appl. Catal. A: Gen. 235 (2002) 171-180.

[15] G. Berhault, M. Lacroix, M. Breysse, F. Maugé, J.-C. Lavalley, H. Nie, L. Qu, J. Catal. 178 (1998) 555-565.
[16] S. M. A. M. Bouwens, F. B. M. Vanzon, M.P. Vandijk, A.M. Vanderkraan, V. H. J. Debeer, J. A. R. Vanveen, D.C. Koningsberger, J. Catal. 146 (1994) 375-393.
[17] J. Ramirez, S. Fuentes, G. Díaz, M. Vrinat, M. Breysse, M. Lacroix, Appl. Catal. 52 (1989) 211-223.
[18] R. Munirathinam, D. Laurenti, G.D. Pirngruber, D. Uzio, ChemistrySelect 2 (2017) 2373-2382.
[19] J. Wu, L. Zhang, Y. Wang, Y. Long, H. Gao, X. Zhang, N. Zhao, Y. Cai, J. Xu, Langmuir 27 (2011) 13684-13691.
[20] H. Lee, S.M. Dellatore, W.M. Miller, P.B. Messersmith, Science (New York, N.Y.) 318 (2007) 426-430.
[21] Y. Liu, K. Ai, L. Lu, Chem. Rev. 114 (2014) 5057-5115.
[22] G. Magendie, B. Guichard, D. Espinat, Catal. Today 258 (2015) 304-318.
[23] W. Zheng, H. Fan, Le Wang, Z. Jin, Langmuir 31 (2015) 11671-11677.
[24] B.A. Morrow, A.J. McFarlan, J. Non-Cryst. Solids 120 (1990) 61-71.
[25] M. Müller, B. Kessler, Langmuir 27 (2011) 12499-12505.
[26] X. Du, L. Li, J. Li, C. Yang, N. Frenkel, A. Welle, S. Heissler, A. Nefedov, M. Grunze, P.A. Levkin, Adv. Mater. 26 (2014) 8029-8033.
[27] Traditionally volume of adsorbed N2 is normalized by the mass of the materials, but in our case we have normalized by the volume of the material. Because, when reasoning per volume instead of per mass, the gain in the mass of the material upon coating Pdop is neutralized, thereby allowing us to see the precise difference between the bare support and Pdop coated support.
[28] M. Zheng, Y. Shu, J. Sun, T. Zhang, Catal. Lett. 121 (2008) 90-96.
[29] J. Vissers, F. Mercx, S. Bouwens, V. de Beer, R. Prins, J. Catal. 114 (1988) 291-302.
[30] C. Zhao, J. Kong, L. Yang, X. Yao, S.L. Phua, X. Lu, Chem. Commun. 50 (2014) 9672-9675.
[31] K.S. Liang, R.R. Chianelli, F.Z. Chien, S.C. Moss, J. Non-Cryst. Solids 79 (1986) 251-273.
[32] B. Radisavljevic, A. Radenovic, J. Brivio, V. Giacometti, A. Kis, Nat. Nanotechnol. 6 (2011) 147-150.
[33] D. J. C. Yates, J. Phys. Chem. 65 (1961) 746-753.
[34] K. Syres, A. Thomas, F. Bondino, M. Malvestuto, M. Grätzel, Langmuir 26 (2010) 14548-14555.
[35] S.J. Hurst, H.C. Fry, D.J. Gosztola, T. Rajh, J. Phys. Chem. C 115 (2011) 620-630.
[36] P. Faye, E. Payen, D. Bougeard, Stud. Surf. Sci. Catal. 106 (1997) 281-292.
[37] P.A. Nikulshin, V.A. Salnikov, A.V. Mozhaev, P.P. Minaev, V.M. Kogan, A.A. Pimerzin, J. Catal. 309 (2014) 386-396.
[38] A.I. Dugulan, J. van Veen, E. Hensen, Appl. Catal. B: Environ. 142-143 (2013) 178-186.
[39] M. Daage, R.R. Chianelli, J. Catal. 149 (1994) 414-427.
[40] P. Persson, R. Bergström, S. Lunell, J. Phys. Chem. B 104 (2000) 10348-10351.

Supplementary Material

Click here to download Supplementary Material: SI-Applied Catal. A_latest version.docx